Generation of Rituximab Polymer May Cause Hyper-Cross-linking–Induced Apoptosis in Non-Hodgkin's Lymphomas

Nan Zhang, Leslie A. Khawli, Peisheng Hu, and Alan L. Epstein

Abstract

Purpose: Although Rituximab has produced significant tumor regressions in lymphoma patients, only 50% respond. Clinically, it has been shown that the major mechanism of action of Rituximab is antibody-dependent cytotoxicity requiring presentation by Fc-bearing cells. To improve the clinical efficacy of Rituximab for the treatment of $CD20^+$ lymphomas, we now describe a new formulation of Rituximab, which, on direct binding to target, can induce apoptosis.

Methods: In this report, enhanced apoptosis was observed by treating $CD20^+$ lymphoma cells with a new polymer formulation of Rituximab. The polymer was produced by formation of a peptide bond using the sugar moiety of dextran (MW 6,000) to generate a clinically relevant reagent for use *in vivo*.

Results: Comparison of Rituximab with a previously described dimer and the newly generated polymer shows that the polymer induced apoptosis more effectively in $CD20^+$ cells as shown by the terminal deoxyribonucleotidyl transferase–mediated dUTP nick end labeling assay (Rituximab, 3%; dimer, 3%; polymer, 58%). Consistent with these results, the polymer produced marked regression in $CD20^+$ lymphoma xenografts, whereas the dimer and monomer reagents showed little effect. In addition, we were able to show that the level of apoptosis induced in human lymphoma cell lines was in accordance with the extent of both surface CD20 clustering and caspase-3 activation.

Conclusions: These data suggest that hyper-cross-linking–induced apoptosis can be simulated by the use of a dextran polymer of Rituximab, which, when used *in vivo*, can directly kill $CD20^+$ lymphoma cells and improve the clinical efficacy of this important therapeutic for human B-cell lymphomas.

The development and Food and Drug Administration approval of the monoclonal antibody Rituximab has provided physicians with an effective new weapon against Non-Hodgkin's lymphomas. This human-mouse chimeric antibody targets CD20, a common cell surface marker of human malignant B-cell lymphomas [see review by Cartron et al. (1)]. CD20 is a 33 to 35 kDa nonglycosylated protein consisting of four-membrane spanning domains with both NH_2 and COOH termini located within the cytoplasm (2–4). At the present time, no CD20 ligand has been described and CD20 does not display the usual structure of a receptor. Instead, several lines of evidence exist to suggest that CD20 may play a crucial role in the regulation of cell cycle progression in B cells (5) and is associated with the control of Ca^{2+} influx across plasma membranes (6).

Whereas Rituximab treatment has produced tumor regressions in patients with relapsed B-cell non-Hodgkin's lymphoma, 52% of those patients do not respond (7). To understand the differential responses to Rituximab, efforts have been made to investigate the mechanisms underlying the antitumor activity of Rituximab and the relative contributions of each mechanism. In this regard, several mechanisms have been implicated including antibody-dependent cellular cytotoxicity, complement-dependent cytotoxicity, and signaling-induced apoptosis [reviewed by Cartron et al. (1)]. Of these mechanisms, the role of complement-dependent cytotoxicity has been questionable because despite *in vitro* studies that show that Rituximab is able to bind complement and effectively initiate complement-dependent cytotoxicity *in vitro* (8–12) and *in vivo* (13), no correlation between *in vitro* complement sensitivity and therapeutic response has been described (14). However, an increase in complement activation products is observed during Rituximab treatment, which may contribute to clinical side effects seen after the first infusion of antibody (15). Hence, it is clear that complement-dependent cytotoxicity plays some role *in vivo* but its contribution to effective therapy requires further confirmation. Likewise, signaling-induced apoptosis remains controversial because direct binding of Rituximab to $CD20^+$ lymphoma cells fails to induce apoptosis to any significant extent (16). To evoke this mechanism, Rituximab must be hyper-cross-linked either by the binding of goat anti-human/mouse immunoglobulin G

Authors' Affiliation: Department of Pathology, Keck School of Medicine, University of Southern California, Los Angeles, California
Received 3/11/05; revised 5/4/05; accepted 5/20/05.
Grant support: Cancer Therapeutics Laboratories, Inc., Los Angeles, CA.
The costs of publication of this article were defrayed in part by the payment of page charges. This article must therefore be hereby marked *advertisement* in accordance with 18 U.S.C. Section 1734 solely to indicate this fact.
Requests for reprints: Alan L. Epstein, Department of Pathology, Keck School of Medicine, University of Southern California, 2011 Zonal Avenue, HMR 205, Los Angeles, CA 90033. Phone: 323-442-1172; Fax: 323-442-3049; E-mail: aepstein@usc.edu.

doi:10.1158/1078-0432.CCR-05-0554

(IgG) or Fcγ receptor–bearing cells, or by immobilization on plastic *in vitro* (16–19). Hyper-cross-linking of Rituximab redistributes CD20 into Triton X–insoluble cell membrane signaling-processing centers (20, 21), followed by lipid raft clustering and transactivation of Src-family tyrosine kinases such as *Lyn*, *Fyn*, and *Lyc*, which further lead to apoptosis of the lymphoma cells (19, 22–24). Only antibody-dependent cellular cytotoxicity, specifically Fc:Fc receptor interaction, is now regarded as a predominant effector mechanism of Rituximab (25, 26). Fcγ receptors on effector cells seem to be responsible for the *in vivo* activity of anti-CD20 antibodies in mice as evidenced by the use of knockout mouse models in which it has been shown that Fc:Fc receptor interaction is required for the depletion of circulating and extravasated B lymphocytes (25). Current clinical studies are focusing on a dimorphism of the *FCGR3A* gene that encodes Fcγ receptor IIIa with either a phenylalanine or a valine at residue 158 which specifically reacts with the lower hinge region of IgG1 with different affinities (phenylalanine > valine; refs. 27–29). It is observed that homozygous FCGR3A-158V patients have a greater probability of experiencing clinical responses, supporting the critical function of the Fc:Fc receptor interaction (27, 29). For antibody-dependent cellular cytotoxicity to be effective, it is assumed that Fc receptor–bearing cells must enter the tumor microenvironment to come in direct contact with its target. If so, then Fc receptor–bearing cells may function as mediators of antibody-dependent cellular cytotoxicity and hyper-cross-linking–induced apoptosis to destroy the tumor. A lack of tumor-associated effector cells may therefore be responsible for Rituximab failure if these mechanisms are critical in patients. If this is the case, the availability of a Rituximab-like reagent to induce apoptosis directly on binding to the surface of $CD20^+$ lymphoma cells would provide a more potent reagent for clinical use.

Recognizing that hyper-cross-linking *in vivo* is impractical, Ghetie et al. (30) reported that tetravalent homodimers of Rituximab could induce higher apoptosis rates in human malignant lymphoma cell lines compared with monomer preparations obtained from the pharmacy. In their studies, they were able to produce apoptosis rates comparable to those obtained by goat anti-mouse hyper-cross-linking and, when tested in combination with chemotherapeutic agents such as doxorubicin, homodimer preparations produced significantly better tumor cell killing. These promising results suggested that an increased valency of Rituximab could initiate apoptosis in the absence of Fc-receptor–bearing cells and may be a method of improving the clinical efficacy of Rituximab therapy. Although *in vivo* data were lacking, this report stimulated the current study in which we tested a new formulation of Rituximab that consisted of a high valency reagent produced by the conjugation of Rituximab to a dextran polymer. When tested both *in vitro* and *in vivo*, this new polymer formulation was found to be a more potent inducer of apoptosis than monomer or dimer preparations. Because of its soluble characteristics, Rituximab polymer is a clinically relevant reagent and has shown good tumor targeting and therapeutic potential in $CD20^+$ Raji xenografts. It is our belief that this newly formulated Rituximab may provide a significant improvement in anti-CD20 therapy, especially in patients with low-affinity Fcγ receptor allotypes.

Materials and Methods

Antibodies

Rituxamab (Rituxan, Genentech, Inc., San Francisco, CA) was purchased from the University of Southern California Norris Cancer Center Pharmacy; goat anti-human IgG (Fc specific) was purchased from Caltag Laboratories (Burlingame, CA); FITC-labeled goat anti-mouse $F(ab')_2$ was purchased from ICN-Cappel (Aurora, OH); and phycoerythrin-labeled anti-CD20 antibody was purchased from BD PharMingen (San Diego, CA). Isotype control antibody, chTV-1, is a mouse human chimeric IgG1 that was developed in our laboratory (31).

Cell lines

Raji, B35M, Ramos, Chevallier, and DG-75 cell lines were obtained from the American Type Culture Collection (Manassas, VA). Farage and Granda 519 cell lines were purchased from Deutsche Sammlung von Mikroorganismen und Zellkulturen GmbH (German Collection of Microorganisms and Cell Cultures, Braunschweig, Germany). The SU-DHL-4, SU-DHL-6, SU-DHL-10, and SU-DHL-16 cell lines were established in our laboratory (32). All cell lines were grown in RPMI 1640 (Life Technologies, San Diego, CA) supplemented with 10% characterized FCS (Hyclone, Logan, UT), 1% glutamine, and penicillin (100 units/mL) and streptomycin (100 μg/mL; Gemini Bio-Products, Woodland, CA), and cultured in a humidified 5% CO_2 incubator at 37°C as stationary suspension cultures.

Conjugation of antibodies to Dynabeads

Rituximab was coated on Dynabeads M-280 Tosylactivated (Dynal Biotech, Inc., Brown Deer, WI) according to the protocol of the manufacturer to study the hyper-cross-linking effect of Rituximab on Raji cells. Briefly, 7×10^8 Dynabeads were washed twice with PBS and incubated with continuous rotation with 200 μg of Rituximab or isotype control antibody in 500 μL at 30°C for 18 to 20 hours. Dynabeads were subsequently pelleted using the magnetic bead attractor (Dynal Biotech), and the unconjugated antibody in the supernatant was quantified by measuring absorbance at 280 nm with a UV spectrophotometer (Ultraspec 2000, Pharmacia, Piscataway, NJ). The total amount of antibody conjugated to the Dynabeads was calculated by the equation (total antibody − unconjugated antibody = conjugated antibody on the beads). Dynabeads coated with antibodies were washed twice with PBS and 1% (w/v) bovine serum albumin (BSA), and free tosyl groups were then treated with blocking solution [0.2 mol/L Tris-HCl (pH 8.5), 0.1% BSA] at 37°C for 3 to 4 hours using end-to-end rotation, washed twice with PBS (0.1% BSA, 1% Tween 20), followed by another two washes with PBS (0.1% BSA). Finally, Dynabeads conjugated with antibodies were resuspended in PBS and stored at 4°C.

Generation of dextran-Rituximab polymer

One-hundred-milligram dextran (average MW 6,000; Fluka Chemie AG, Buchs, Switzerland) and 120 mg sodium periodate (Sigma, St Louis, MO) were dissolved in 5 mL of 0.9% NaCl solution and incubated for 18 hours in the dark at room temperature. The mixture was passed through a preequilibrated PD-10 column (Amersham Biosciences, Piscataway, NJ), eluted in 0.9% NaCl, and stored at 4°C in the dark. Two milliliters of Rituximab (10 mg/mL) were passed through a preequilibrated PD-10 column and eluted with 0.1 mol/L sodium bicarbonate buffer (pH 8.1; Sigma). The eluted Rituximab was diluted to 5 mg/mL with 0.1 mol/L sodium bicarbonate buffer (pH 8.1), and mixed with 480 μg oxidized dextran at a molar ratio of 1:2.4 (Rituximab/oxidized dextran). After continuous shaking for 6 hours in the dark, the reaction was reduced with 5 mg sodium borohydride (Sigma) for 1 hour followed by dialysis in PBS. The dialysate was then passed through a 0.22 μm nonpyrogenic syringe filter (Costar, Corning, NY), and a Pharmacia AKTA System (fast protein liquid chromatography; Amersham Pharmacia Biotech, Piscataway, NJ) was used to fractionate the dextran Rituximab mixture through a preequilibrated Superose 6 column in PBS at a flow rate of 0.5 mL/min. The polymer

had a retention time of ~16 minutes. The polymer fraction was further concentrated using Centricon YM-100 (Millipore, Billerica, MA), sterilized by 0.22 μm filtration, and analyzed by SDS-PAGE and agarose electrophoresis. Proteins were analyzed under nonreducing conditions by SDS-PAGE on a 4% stacking, 5% separating gel and a 2% agarose gel. Protein bands were visualized by Coomassie blue staining.

Generation of Rituximab homodimer

Two heterobifunctional cross-linkers, *N*-succinimidyl *S*-acethylthioacetate (SATA; Pierce, Rockford, IL) and succinimidyl 4-(maleimidomethyl) cyclohexane-1-carboxylate (SMCC; Pierce), were used to generate homodimers of Rituximab with modifications (30, 33).

Step 1: ***Derivatization with succinimidyl 4-(maleimidomethyl) cyclohexane-1-carboxylate.*** Five milligrams of Rituximab at a concentration of 5 mg/mL in 0.05 mol/L phosphate buffer containing 3 mmol/L Na_2EDTA (PBE; pH 7.5) and 2.5 μL of SMCC (9.3 mg/mL DMSO) were incubated with continuous rotation at room temperature for 1 hour using a SMCC/Rituximab molar ratio of 4.5. Conjugated protein was purified by chromatography on a PD-10 column in PBE buffer.

Step 2: ***Derivatization with N-succinimidyl S-acethylthio-acetate.*** Five milligrams of Rituximab (5 mg/mL PBE) were mixed with 2.5 μL of SATA (5.8 mg/mL DMSO) and incubated at room temperature for 1 hour using a SATA/Rituximab molar ratio of 4.0. The excess SATA was then removed by chromatography on a PD-10 column and the purified protein was deacetylated with 5 mg of hydroxylamine-HCl (Sigma) for 5 minutes at room temperature. Excess hydroxylamine-HCl was removed by chromatography on a PD-10 column.

Step 3: ***Reaction of SMCC- and SATA-derived rituximab.*** SMCC- and SATA-derived proteins were mixed together and incubated with continuous rotation at room temperature for 1 to 2 hours. The preparation was dialyzed overnight in PBS at 4°C, sterilized by filtration through a 0.22 μm nonpyrogenic filter (Costar), and further fractionated on a Superose 6 Column using the Pharmacia AKTA described above at flow rate of 0.5 mL/min. The dimer had a retention time of ~29 minutes. The protein fractions purified by fast protein liquid chromatography were further concentrated using Centricon YM-100, filter sterilized, and analyzed by SDS/PAGE as described above.

In vitro Studies

Serum stability. *In vitro* serum stability was evaluated using an immunoblotting assay. Briefly, Rituximab polymer was incubated for up to 10 days in goat serum at 37°C. At different times after incubation, samples were separated by SDS-PAGE and transferred to a polyvinylidene difluoride membrane. A horseradish peroxidase–conjugated polyclonal goat anti-human IgG (Fc specific) was used to detect the human Fc portion of Rituximab.

CD20 expression determination. CD20 expression was determined by fluorescence-activated cell sorting analysis using anti-CD20 antibody labeled with phycoerythrin as previously described (11).

Rituximab avidity constant determination. Rituximab monomer, dimer, and polymer were radiolabeled with radioiodine using a modified chloramine-T method developed in our laboratory (34). To determine the avidity constant of each Rituximab preparation, a fixed cell RIA was done using the method of Frankel and Gerhard (35) as previously described. The avidity constant K_a was calculated by the equation $K = -(\text{slope}/n)$, where n is the valence of the antibody ($n = 2$ for the monomer; $n = 4$ for the dimer; $n = 10$ for the polymer).

Apoptosis induction and detection. (*a*) Annexin V/propidium iodide staining. Two micrograms of Rituximab monomer, dimer, and polymer, and Rituximab-conjugated Dynabeads (equivalent to 2 μg) were added to 5×10^4 Raji cells in 200 μL media and incubated for 18 hours in a 5% CO_2 incubator at 37°C. For hyper-cross-linking, 5×10^4 Raji cells in 200 μL media were incubated with 2 μg of Rituximab for 1 hour at 37°C. The cells were then washed twice with PBS (1% BSA) and then incubated with 5 μg of goat anti-human antibody (Caltag) for 18 hours at 37°C in a 5% CO_2 incubator. The percentage of apoptosis induced by each antibody preparation was then determined by the Annexin V/propidium iodide staining assay, which directly detects phosphotidylserine exposure on apoptotic cells and the loss of the cellular membrane integrity. Annexin V and propidium iodide stainings were done using the RAPID protocol provided by the manufacturer (Oncogene Research Product, Boston, MA).

(*b*) Terminal deoxyribonucleotidyl transferase–mediated dUTP nick end labeling (TUNEL) assay. Induction of DNA strand breaks by each antibody preparation was determined by the TUNEL assay using an APO-DIRECT Kit (Phoenix Flow Systems, San Diego, CA) following the protocol of the manufacturer. For these studies, 5×10^5 Raji cells were incubated with each antibody preparations (20 μg) in 1.5 mL for 18 hours at 37°C in a 5% CO_2 incubator. For the hyper-cross-linking studies, 5×10^5 Raji cells were incubated with 20 μg of Rituximab in 1.5 mL for 1 hour at 37°C. Cells were then washed twice with PBS and further incubated with 50 μg of goat anti-human antibody (Caltag) in 1.5 mL for 18 hours at 37°C in a 5% CO_2 incubator. The cells were then washed with PBS, fixed in 2% paraformaldehyde at room temperature, and permeabilized in 70% ethanol for storage overnight at −20°C.

Caspase-3 activity assays. Two micrograms of Rituximab monomer, dimer, and polymer, and Rituximab- and isotype control antibody–conjugated Dynabeads were incubated with 5×10^4 Raji cells. After 5 and 24 hours, the cells were washed with PBS, resuspended in 40 μL of the fluorogenic protease substrate Phiphilux (OncoImmunin, Inc., Gaithersburg, MD), and incubated in a 30°C water bath for 40 minutes. Lastly, the cells were resuspended in media provided by the manufacturer and immediately analyzed by flow cytometry.

Immunofluorescence microscopy. The pattern of antigen cross-linking on the surfaces of cells treated with different antibody preparations was observed by immunofluorescence microscopy. For these studies, 5×10^5 Raji cells were treated with 20 μg of each antibody preparations at 37°C, fixed with 2% paraformaldehyde (Polysciences, Inc., Warrington, PA), diluted in PBS at room temperature, followed by two washes with PBS (1% BSA). Fixed cells were then incubated with 25 μg of goat anti-mouse antibody $F(ab')_2$ (ICN-Cappel) at 4°C for 30 minutes and subsequently washed twice with PBS (1% BSA). For the hyper-cross-linking studies by a secondary goat-anti-mouse IgG $F(ab')_2$, 5×10^5 Raji cells were treated with 20 μg of Rituximab for 1 hour at 37°C. The cells were washed with PBS twice and incubated with 25 μg of goat anti-mouse antibody $F(ab')_2$ for 30 minutes at 4°C. Cells were then washed twice and fixed as above. Cytospin preparations were mounted in Vectorshield with 4′,6-diamidino-2-phenylindole (Vector Laboratories, Burlingame, CA) for observation under a phase-contrast fluorescence microscope using a 50× water immersion lens.

In vivo studies

Pharmacokinetic and biodistribution studies. Six-week-old female athymic nude mice were used to determine the pharmacokinetic clearance of the radiolabeled Rituximab monomer, dimer, and polymer preparations as previously described (34, 36). Significance levels (P values) were determined using the Wilcoxon rank-sum test.

Tissue biodistribution studies were done in Raji tumor–bearing nude mice to examine the targeting ability of the Rituximab monomer, dimer, and polymer. Six-week-old female athymic nude mice (Harlan, Indianapolis, IN) were irradiated with 350 rad from a cesium source to suppress innate natural killer activity, and 3 days later were injected s.c. with a 0.2 mL inoculum containing 5×10^6 Raji lymphoma cells and 10^5 human fetal fibroblast feeder cells in the left flank using a University Animal Care Committee–approved protocol. The human fetal fibroblast feeder cells established in our laboratory provide growth factors that promote a high tumor take rate (>90%). Tumors were grown for 10 to 15 days until they reached 0.5 cm in diameter. In each group ($n = 5$), individual mice were injected i.v. with a 0.1 mL inoculum containing 30 to 40 μCi of ^{125}I-labeled antibody preparations. Mice were then sacrificed by sodium pentobarbital overdose at 72 hours postinjection, and tissues were removed, weighed, and

measured in a γ counter. For each mouse, data were expressed as percentage injected dose per gram (% ID/g) and as tumor/organ ratio (cpm per gram tumor/cpm per gram organ). Significance levels were determined using a Wilcoxon's rank-sum test.

Immunotherapy studies. Six-week-old female athymic nude mice were heterotransplanted with Raji lymphoma cells as described above. When tumors reached 0.5 cm in diameter, groups of mice (n = 5) were injected i.v. with 0.1 mL inoculum containing 25 μg of the Rituximab monomer, dimer, or polymer. All groups were treated every other day five times and tumor volumes were monitored thrice a week by caliper measurement in three dimensions using the formula length × width × height. All data were presented as means of tumor volume (cm^3) and significance levels were determined using the Wilcoxon's rank-sum test. All mice were sacrificed by sodium pentobarbital overdose.

Results

Direct induction of apoptosis by Rituximab preparations

Raji lymphoma cells were treated with Rituximab alone or hyper-cross-linked Rituximab for 18 to 20 hours at 37°C. The amount of apoptosis was measured by Annexin V/propidium iodide staining (Fig. 1A), which detects phosphotidylserine exposure on the extracellular membrane and loss of membrane integrity, and by TUNEL assay (Fig. 1B), which quantitates DNA strands breaks, a phenomenon downstream of endonuclease activation. In addition to Rituximab hyper-cross-linked with traditional secondary goat anti-human antibody, Rituximab was

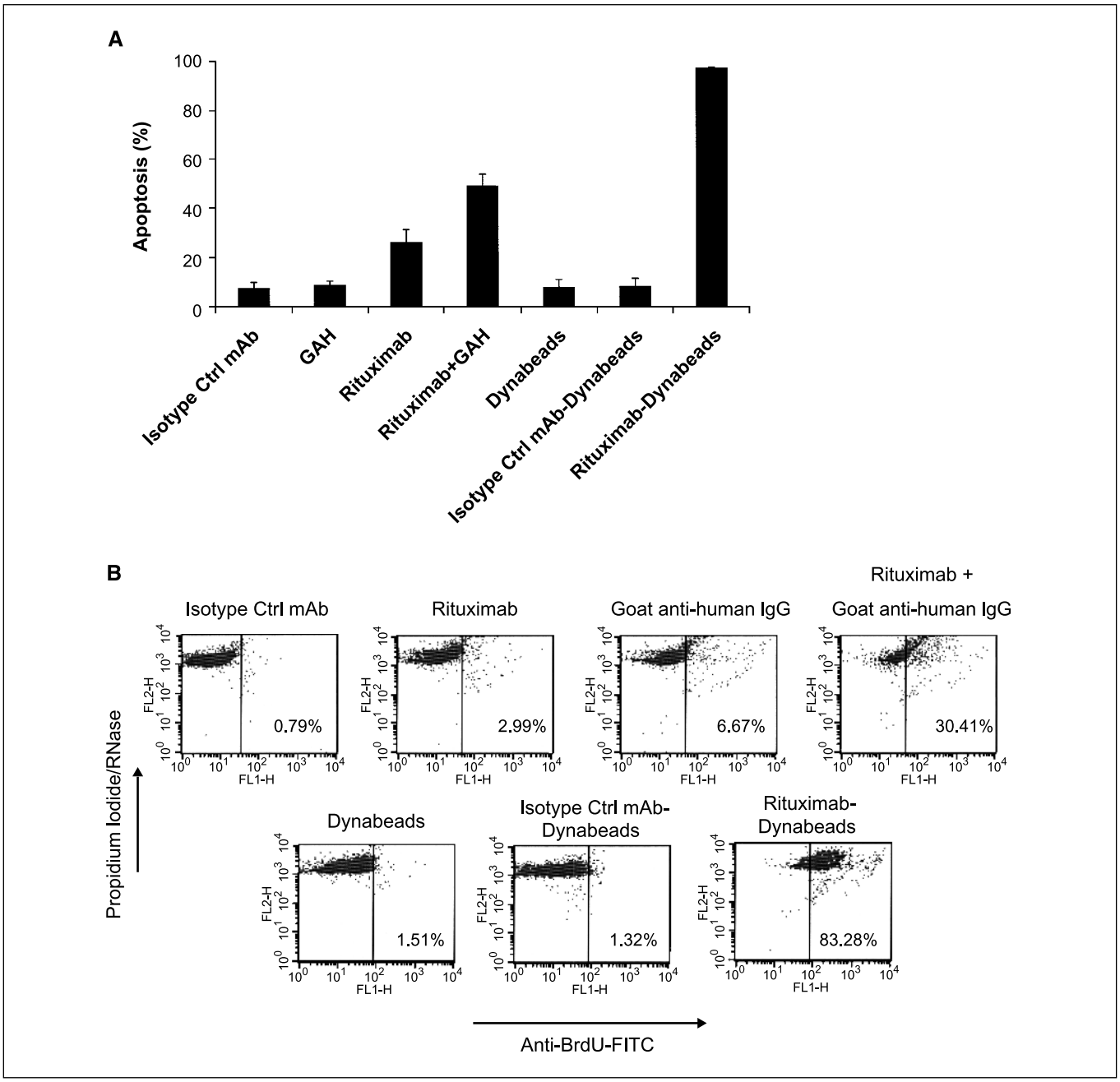

Fig. 1. Rituximab hyper-cross-linking – induced apoptosis of Raji lymphoma cells as assessed by Annexin V/propidium iodide staining (*A*) and TUNEL assay (*B*).

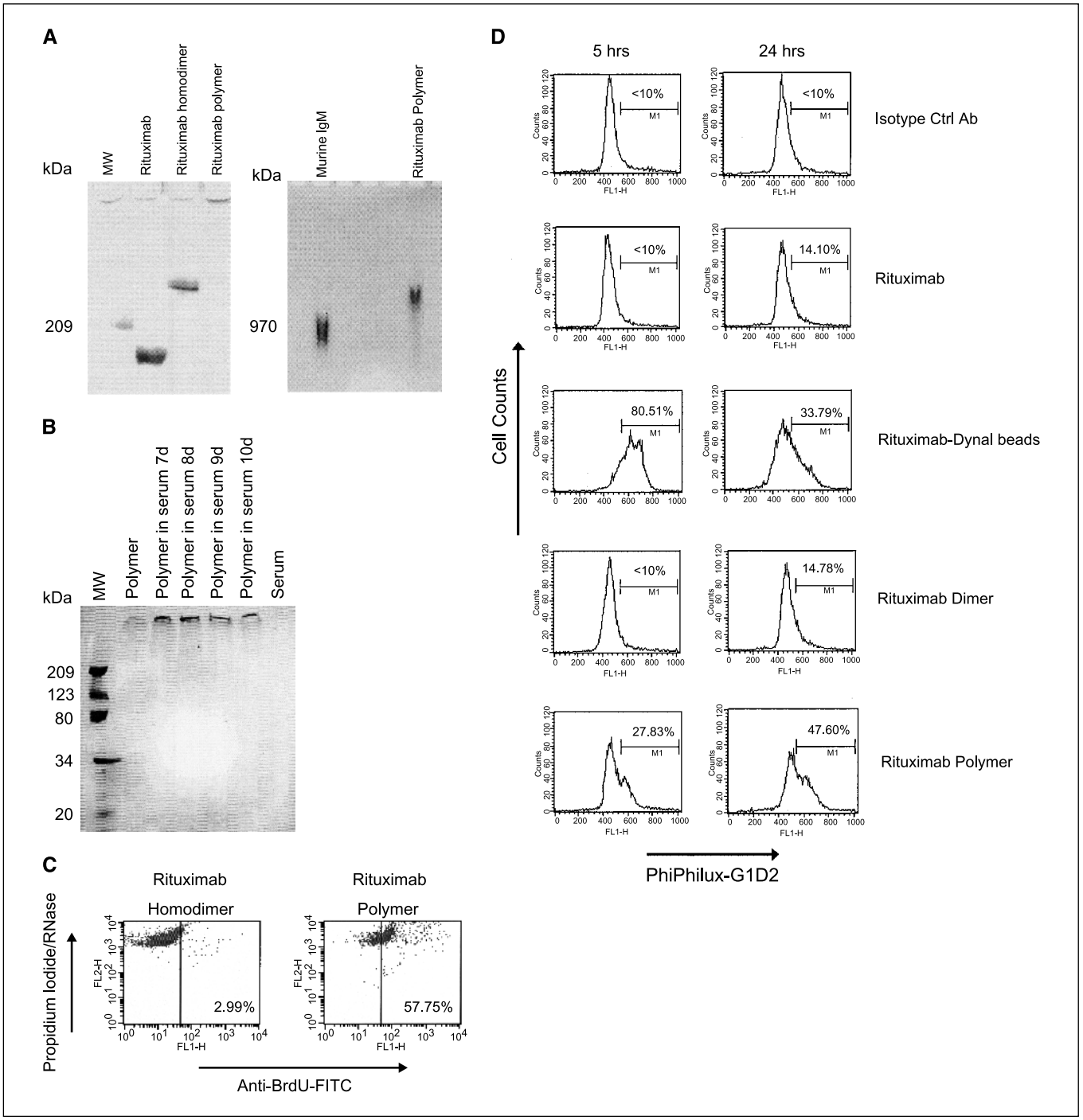

Fig. 2. Analysis of Rituximab polymer and dimer preparations. *A,* electrophoretic analysis of Rituximab dimer and polymer using 4% to 15% nonreducing SDS-PAGE (*left*) and 2% agarose (*right*). *B,* immunoblotting assay of Rituximab polymer incubated in serum over a 10-day period at 37°C. *C,* TUNEL assay demonstrating apoptosis of Raji lymphoma cells induced by Rituximab dimer and polymer. *D,* fluorescence-activated cell sorting analysis of caspase-3 activation in Raji lymphoma cells following treatment with different Rituximab preparations. Baseline values are shown on top in which data are presented for the isotype control antibody.

also conjugated to Tosyl-activated Dynabeads (2.8 μm in diameter) to simulate *in vitro* Fc presentation of antibody by Fc-receptor–bearing cells (Fig. 1). These studies showed that Rituximab alone induced only a minimal level of apoptosis in Raji cells (26% in the Annexin V assay and 2.99% in the TUNEL assay). By comparison, Rituximab hyper-cross-linked with goat anti-human antibody caused a higher level of apoptosis (50% in the Annexin assay and 30% in the TUNEL assay). Interestingly, Rituximab conjugated to Dynabeads was found to induce the best apoptosis levels detected by both Annexin V/propidium iodide staining and TUNEL assays (96% and 83%, respectively).

Generation and characterization of Rituximab dimer and polymer

SATA and SMCC were used to generate homodimers of Rituximab following the method developed by Ghetie et al.

(30, 33). To prevent precipitation of Rituximab dimers in the chemical reaction, the concentration of Rituximab used was decreased from 10 to 5 mg/mL. Rituximab polymer was generated using aldehyde-activated dextran (average M_r 6,000). Both the Rituximab homodimer and polymer preparations were dialyzed overnight and fractionated using a fast protein liquid chromatography. The polymer revealed a retention time of ~16 minutes whereas the dimer revealed a retention time of ~29 minutes by fast protein liquid chromatography. The purity of each preparation was >99%. The molecular weights of the Rituximab polymer and dimer were shown by nonreducing SDS-PAGE (Fig. 2A). Under these conditions, the molecular weight of the polymer was found to be beyond the SDS-PAGE measurement capabilities due to the fact that the polymer did not enter the gel. To solve this problem, a 2% agarose gel was used along with murine immunoglobulin M, which has a known molecular weight of 970 kDa (Fig. 2A). By this method, one band was resolved for the Rituximab polymer, which was slightly higher than that of immunoglobulin M, corresponding to the molecular weight of ~5 immunoglobulin molecules. Additional studies are under way to determine the degree of heterogeneity of the polymer.

In vitro studies

Serum stability. Rituximab polymer was examined for stability in goat serum over a 10-day incubation period at 37°C. The result showed no degradation over this time period (Fig. 2A) or over a 6-month incubation period at 4°C.

Avidity studies. Avidity binding studies were conducted in which ^{125}I-labeled Rituximab preparations were incubated with Raji lymphoma cells and the bound radioactivity was used to calculate the avidity constant (K_a) by Scatchard analysis. Using this method, the Rituximab polymer was found to have an avidity constant of 3.16×10^8 $(mol/L)^{-1}$, whereas the monomer and dimer had avidity constants of 3.6×10^8 and 2.09×10^8 $(mol/L)^{-1}$, respectively. These studies show that the Rituximab polymer and dimer have similar binding avidities to antigen as Rituximab monomer, facilitating subsequent direct comparisons *in vitro* and *in vivo*.

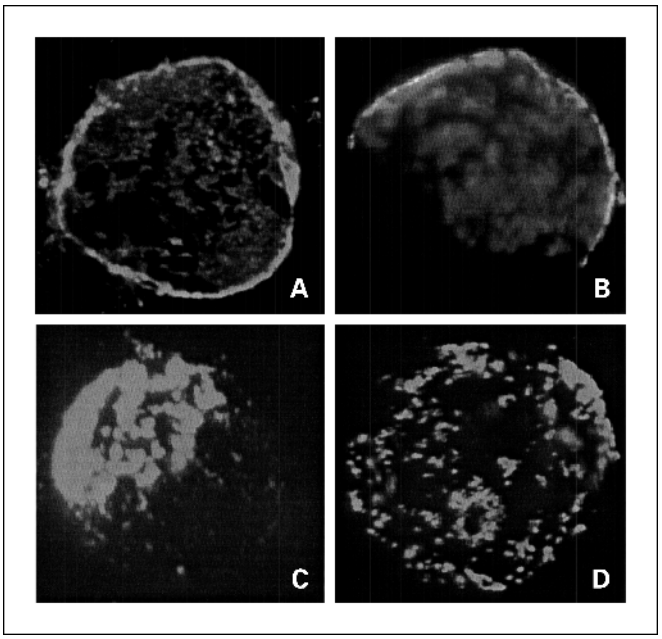

Fig. 3. Extent of CD20 clustering on Raji cell surface shown by immunofluorescence microscopy. Cells were treated with Rituximab monomer (*A*), dimer (*B*), or polymer (*C*), and then fixed with 2% paraformaldehyde and stained with a secondary goat anti-mouse IgG-FITC. *D,* cells were treated with Rituximab and secondary goat anti-mouse IgG-FITC, followed by fixation with 2% paraformaldehyde. Results show ring patterns of staining with Rituximab monomer and dimer but more speckled and segregated polar staining patterns with polymer and Rituximab + goat anti-mouse antibody.

Induction of apoptosis by Rituximab dimer and polymer. Apoptosis assays were used to analyze the ability of the Rituximab polymer and dimer to induce apoptosis. TUNEL assays showed that the Rituximab polymer induced 57.8% apoptosis whereas the dimer produced only 2.99% (Fig. 2C).

Table 1. Induction of apoptosis in CD20$^+$ and CD20$^-$ cell lines by Rituximab monomer, dimer, and polymer preparations

Lymphoma cell lines	CD20 expression (MFI*)	Untreated	Rituximab	Rituximab dimer	Rituximab polymer
CD20$^+$					
Raji	514.34	4.56†	27.86	26.97	66.07
B35M	349.33	6.02	13.13	8.92	56.36
RAMOS	374.44	5.04	7.66	6.08	24.68
SU-DHL-4	672.19	4.78	10.67	7.31	11.54
SU-DHL-6	685.64	28.16	45.36	42.50	55.89
SU-DHL-10	631.97	7.01	27.85	25.69	36.88
SU-DHL-16	585.14	15.07	27.28	23.06	31.43
Farage	643.63	19.22	21.25	20.56	46.11
Granda 519	495.48	11.78	20.27	18.61	48.30
Chevallier	408.99	18.18	18.80	16.80	40.70
CD20$^-$					
DG-75	180.78	6.82	8.04	6.85	7.85
L540	196.37	16.23	16.54	16.02	16.00

*Mean fluorescence intensity.
†Percent nonviable cells.

To investigate whether these results would be similar with other human malignant lymphoma cell lines, 12 different cell lines were studied including 10 $CD20^+$ and 2 $CD20^-$ (Table 1). In the $CD20^+$ cell lines, apoptosis was significantly increased in the cells treated with Rituximab polymer compared with those treated with the dimer or monomer. However, not all $CD20^+$ cells treated with Rituximab polymer showed significant apoptosis. It is assumed that some of these lymphoma cell lines may have different intracellular pathways associated with CD20 ligation. As expected, no significant apoptosis was detected in any of the $CD20^-$ cell lines treated with the different Rituximab preparations.

Caspase-3 activation studies. As shown in Fig. 2D, Raji lymphoma cells treated with Rituximab monomer or dimer were found to have basal levels of caspase-3 activity similar to controls. By contrast, Raji cells treated with Rituximab polymer or Rituximab-coated Dynabeads showed significant caspase-3 activation. For polymer treated cells, caspase-3 activity started to elevate at 5 hours after treatment and reached a peak at 24 hours. For those cells treated with Rituximab-coated Dynabeads, caspase-3 activity peaked at 5 hours after treatment and declined at 24 hours. From these experiments, it seems that early induction of apoptosis correlated with a more vigorous activation of caspase-3 as seen with the samples treated with Rituximab-coated Dynabeads.

Immunofluorescence microscopy studies. To investigate further whether there is any correlation between surface hyper-cross-linking of CD20 and apoptosis, immunofluorescence

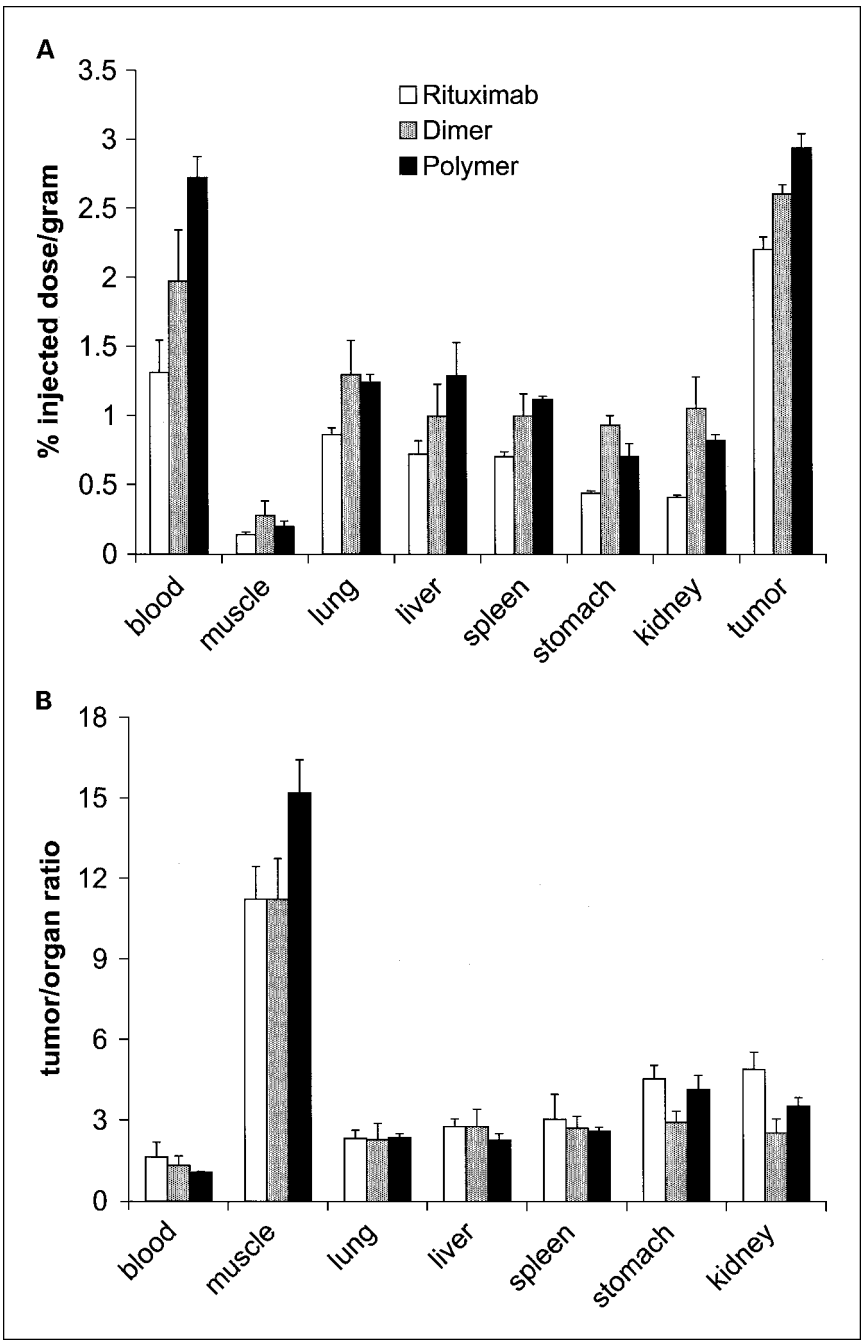

Fig. 4. Tissue biodistribution and tumor uptake of Rituximab polymer, dimer, and monomer at 72 hours postinjection in Raji lymphoma – bearing nude mice. *A,* tumor uptake measured by percent injected dose per gram of ^{125}I-labeled Rituximab polymer, dimer, or monomer. *B,* tumor/normal organ ratios; columns, mean; bars, SD.

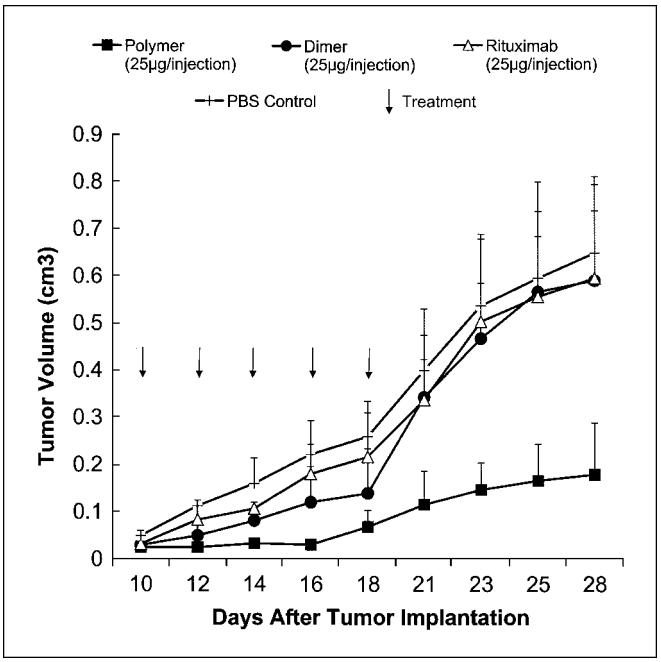

Fig. 5. Rituximab polymer, dimer, and monomer immunotherapy in Raji xenograft model.

staining was done to study the Rituximab and CD20 antigen distribution on the cell surface. As shown in Fig. 3, Rituximab monomer and dimer treatments produced a ring pattern of immunofluorescence, indicating that CD20 is evenly distributed on the surface of the lymphoma cells. By contrast, cells treated with Rituximab polymer or Rituximab + goat anti-mouse antibody were found to have a more segregated polar staining pattern consistent with the movement and fixation of CD20 into lipid rafts.

In vivo studies

Pharmacokinetic and biodistribution studies. Whole-body radioactivity studies in athymic nude mice showed that radiolabeled Rituximab had a $T_{1/2}$ of 96 hours ($P < 0.01$) whereas the dimer and polymer had half-lives of 120 and 144 hours, respectively ($P < 0.01$). These results are consistent with prior data showing polymeric antibodies to have longer half-lives than native antibodies (37). As shown in Fig. 4, biodistribution studies with all three Rituximab preparations illustrate effective localization to the Raji xenografts resulting in approximately similar tumor-to-organ ratios. The data further show the specificity of tumor targeting with all three Rituximab preparations as indicated by the high tumor uptake observed.

Immunotherapy studies. As shown in Fig. 5, the antitumor activity of the Rituximab preparations was studied in Raji tumor–bearing nude mice. As described above, treatment did not commence until day 10 when the tumors were palpable in size. In those groups of mice receiving the monomer or dimer, tumor growth was either unaffected or slightly slower than that seen in the untreated control group. By contrast, the group of mice receiving the polymer treatment showed marked tumor regression (Fig. 5). These results show that the average tumor volume of the polymer-treated group on the 28th day after tumor implantation was <30% of the tumor volume in the PBS-treated control group ($P < 0.01$). These findings are notable in view of the fact that all these preparations had comparable avidity constants and biodistribution characteristics in this same tumor model.

Discussion

As previously shown (16–19), direct induction of apoptosis by Rituximab is very ineffective unless the antibody is hyper-cross-linked by secondary antibody or immobilized on plastic. The goal of the present work was to determine if higher valency preparations of Rituximab could be used to simulate hyper-cross-linking events using formulations that are applicable *in vivo*. This goal was achieved by the generation of a polymer of Rituximab that consisted of ~5 immunoglobulins per dextran molecule. To show its potency *in vitro* and *in vivo*, the polymer preparation was compared with Rituximab monomer and with a previously published dimer (30), which showed some improved activity when tested in apoptosis assays. Our results clearly showed that the polymer is able to induce apoptosis of $CD20^+$ human lymphoma cell lines directly on binding, distinguishing it from both the monomer and dimer preparations using the TUNEL assay (Rituximab, 3%; dimer, 3%; polymer, 58%; see Figs. 1B and 2B). These findings were obtained despite the fact that all three preparations had essentially equal avidity constants against CD20 antigen and had similar pharmacokinetic properties and biodistribution characteristics in tumor-bearing nude mice. In addition, the Rituximab polymer was found to be much more effective *in vivo* against implanted Raji lymphomas using dosages in which the monomer and dimer preparations had little effect. In contrast to the results of Ghetie et al. (30), the dimer preparation produced in our laboratory (99% pure) induced no noticeable increase in apoptosis *in vitro*. This may have been due to the presence of polymers contaminating their dimer preparations, which were reported to be only 80% pure.

In this report, various methods of CD20 hyper-cross-linking–induced apoptosis were quantified by both Annexin V and TUNEL assays. Of note, Rituximab-coated Dynabeads induced maximum levels of apoptosis in Raji cells in which >90% of cells were shown to become apoptotic. Several factors may have contributed to the induction of such a high apoptosis percentage. First, Rituximab was conjugated to Dynabeads by peptide bonding which produced a more rigid presentation of antibody to the lymphoma cells than that obtained with secondary antibodies or plastic substrata. Second, the Dynabeads have a rounded surface, allowing multiple contact points to facilitate maximum interaction with target, and are small enough to have several beads attach to each target cell. Under the microscope, the Rituximab-coated Dynabeads often produced cell aggregation due to their attachment to multiple lymphoma cells. Finally, a high concentration of antibody was attached to the beads providing an optimal binding surface for cross-linking. By contrast, Rituximab immobilized to a plastic surface or hyper-cross-linked with secondary antibody either has a limited interactive interface or is not as efficient in fixing CD20 in hydrophobic regions once the CD20 has migrated into the lipid rafts, the latter being a requirement for optimal induction of apoptosis according to data presented by Deans et al. (38), but not according to the data of Chan et al. (39). Because of these results, we hypothesize that the Dynabead presentation is

more likely to be that obtained with Fc receptor–bearing cells *in vivo*. Regardless, antibody-coated Dynabeads may represent a new and simple method for identifying antibodies and antigens in which apoptosis induction via Fc receptor–bearing cell presentation is an important mechanism of action.

To further investigate whether there is any correlation between surface hyper-cross-linking of CD20 and apoptosis, immunofluorescence staining was done to study antibody and antigen distribution on the cell surface. As shown in Fig. 3, treatment with Rituximab monomer and dimer produced a ring pattern of staining, indicating that these reagents reacted with antigen that was evenly distributed on the surface of the cell. By contrast, those cells treated with Rituximab polymer or hyper-cross-linked with secondary antibody showed a more segregated polar staining pattern, a finding which correlated with higher apoptosis induction and the movement of antigen into lipid rafts (38). From these experiments, we concluded that CD20 antigen clustering is associated with superior induction of apoptosis and that immunofluorescence microscopy is a good method for observing the effects of various antibody preparations on the induction of apoptosis.

As described above, many mechanisms have been proposed to explain the effectiveness of Rituximab treatment both in animal models and man. The notion that antibody-dependent cellular cytotoxicity plays a major role *in vivo* is the current prevailing hypothesis and several articles have already addressed the importance of antibody presentation via Fc receptors (25, 26, 29). In mouse models, Fcγ receptor II has an inhibitory role in the therapeutic effect of Rituximab (26), but some studies produced contradictory results (40). Specifically, mouse fibroblast Ltk− cells that were transfected with Fcγ receptor II still facilitated signaling-induced apoptosis (16). In the present study, the fact that the polymer preparation effectively suppressed Raji lymphoma growth *in vivo* emphasizes the point that apoptosis alone can be a powerful mechanism for treating lymphomas. In support of this concept, clinical studies by Byrd et al. (41) found caspase-3 cleavage in lymphoma cells of patients treated with Rituximab as evidence of the induction of apoptosis after treatment. In this situation, apoptosis was most likely due to presentation of antibody via Fc receptor–bearing cells. In our experiments, caspase-3 induction was found to occur with Rituximab-coated Dynabeads and polymer (Fig. 2C). By contrast, Rituximab monomer and dimer treatments produced only basal levels of caspase-3 activity.

In summary, it seems that the induction of apoptosis in lymphoma cells requires proper presentation of anti-CD20 to induce CD20 movement into lipid rafts and subsequent fixation of the antigen in these polar regions of the cell surface. The high valency afforded by the Dynabeads preparation *in vitro* and the polymer preparation *in vivo* may facilitate fixation and trapping (hyper-cross-linking) of CD20 on the cell surface, thereby providing a strong signal to initiate apoptosis pathways resulting in the activation of caspase 3. *In vitro*, amplified apoptosis can be achieved using secondary antibodies, Fc receptor–bearing cells, or Rituximab-coated Dynabeads. *In vivo*, hyper-cross-linking seems to require presentation by Fc receptor–bearing cells (25), a mechanism which apparently can be simulated by the polymer preparation. Not requiring the presence of effector cells for the induction of apoptosis, the polymer preparation may be especially useful in lymphoma patients who have the low Fc receptor phenotype and who are nonresponsive to Rituximab monotherapy (27). Finally, because Rituximab-coated Dynabeads treatment produced >90% apoptosis, it is conceivable that additional formulation work on Rituximab polymers can achieve higher levels, rendering this new form of treatment optimally effective above the current 58% apoptosis rate (*in vitro*) presently obtained.

Acknowledgments

We thank Jingzhong Pang for his expert assistance and diligence with the animal studies, Harold R. Soucier for performing the flow cytometry analyses, and Rebecca Sadun for comments on the manuscript.

References

1. Cartron G, Watier H, Golay J, Solal-Celigny P. From the bench to the bedside: ways to improve Rituximab efficacy. Blood 2004;104:2635–42.
2. Ishibashi K, Suzuki M, Sasaki S, Imai M. Identification of a new multigene four-transmembrane family (MS4A) related to CD20, HTm4 and β subunit of the high-affinity IgE receptor. Gene 2001;264:87–93.
3. Einfeld DA, Brown JP, Valentine MA, Clark EA, Ledbetter JA. Molecular cloning of the human B cell CD20 receptor predicts a hydrophobic protein with multiple transmembrane domains. EMBO J 1988; 7:711–7.
4. Stashenko P, Nadler LM, Hardy R, Schlossman SF. Characterization of a human B lymphocyte-specific antigen. J Immunol 1980;125:1678–85.
5. Golay JT, Clark EA, Beverley PC. The CD20 (Bp35) antigen is involved in activation of B cells from the G_0 to the G_1 phase of the cell cycle. J Immunol 1985;135: 3795–801.
6. Li H, Ayert LM, Lytton J, Deans JP. Store-operated cation entry mediated by CD20 in membrane rafts. J Biol Chem 2003;278:42427–34.
7. McLaughlin P, Grillo-Lopez AJ, Link BK, et al. Rituximab chimeric anti-CD20 monoclonal antibody therapy for relapsed indolent lymphoma: half of patients respond to a four-dose treatment program. J Clin Oncol 1998;16:2825–33.
8. Reff ME, Carner K, Chambers KS, et al. Depletion of B cells *in vivo* by a chimeric mouse human monoclonal antibody to CD20. Blood 1994;83:435–45.
9. Flieger D, Renoth S, Beier I, Sauerbruch T, Schmidt-Wolf I. Mechanism of cytotoxicity induced by chimeric mouse human monoclonal antibody IDEC-C2B8 in CD20-expressing lymphoma cell lines. Cell Immunol 2000;204:55–63.
10. Harjunpaa A, Junnikkala S, Meri S. Rituximab (anti-CD20) therapy of B-cell lymphomas: direct complement killing is superior to cellular effector mechanisms. Scand J Immunol 2000;51:634–41.
11. Golay J, Lazzari M, Facchinetti V, et al. CD20 levels determine the *in vitro* susceptibility to Rituximab and complement of B-cell chronic lymphocytic leukemia: further regulation by CD55 and CD59. Blood 2001;98:3383–9.
12. Bellosillo B, Villamor N, Lopez-Guillermo A, et al. Complement-mediated cell death induced by Rituximab in B-cell lymphoproliferative disorders is mediated *in vitro* by a caspase-independent mechanism involving the generation of reactive oxygen species. Blood 2001;98:2771–7.
13. Di Gaetano N, Cittera E, Nota R, et al. Complement activation determines the therapeutic activity of Rituximab *in vivo*. J Immunol 2003;171:1581–7.
14. Weng WK, Levy R. Expression of complement inhibitors CD46, CD55, and CD59 on tumor cells does not predict clinical outcome after Rituximab treatment in follicular non-Hodgkin lymphoma. Blood 2001;98:1352–7.
15. Van der Kolk LE, Grillo-Lopez AJ, Baars JW, Hack CE, van Oers MH. Complement activation plays a key role in the side effects of Rituximab treatment. Br J Haematol 2001;115:807–11.
16. Shan D, Ledbetter JA, Press OW. Apoptosis of malignant human B cells by ligation of CD20 with monoclonal antibodies. Blood 1998;91:1644–52.
17. Shan D, Ledbetter JA, Press OW. Signaling events involved in anti-CD20-induced apoptosis of malignant human B cells. Cancer Immunol Immunother 2000; 48:673–83.
18. Van der Kolk LE, Evers LM, Omene C, et al. CD20-induced B cell death can bypass mitochondria and caspase activation. Leukemia 2002;16:1735–44.
19. Hofmeister JK, Cooney D, Coggeshall KM. Clustered CD20 induced apoptosis: src-family kinase, the proximal regulator of tyrosine phosphorylation, calcium influx, and caspase 3-dependent apoptosis. Blood Cells Mol Dis 2000;26:133–43.
20. Semac I, Palomba C, Kulangara K, et al. Anti-CD20 therapeutic antibody Rituximab modifies the functional organization of rafts/microdomains of B lymphoma cells. Cancer Res 2003;63:534–40.
21. Polyak MJ, Tailor SH, Deans JP. Identification of a cytoplasmic region of CD20 required for its redistribution to a detergent-insoluble membrane compartment. J Immunol 1998;161:3242–8.
22. Deans JP, Schieven GL, Shu GL, et al. Association

of tyrosine and serine kinases with the B cell surface antigen CD20. Induction via CD20 of tyrosine phosphorylation and activation of phospholipase C-γ1 and PLC phospholipase C-γ2. J Immunol 1993;151:4494–504.

23. Deans JP, Kalt L, Ledbetter JA, Schieven GL, Bolen JB, Johnson P. Association of 75/80-kDa phosphoproteins and the tyrosine kinases Lyn, Fyn, and Lck with the B cell molecule CD20. Evidence against involvement of the cytoplasmic regions of CD20. J Biol Chem 1995;270:22632–8.

24. Deans JP, Robbins SM, Polyak MJ, Savage JA. Rapid redistribution of CD20 to a low density detergent-insoluble membrane compartment. J Biol Chem 1998;273:344–8.

25. Uchida J, Hamaguchi Y, Oliver JA, et al. The innate mononuclear phagocyte network depletes B lymphocytes through Fc receptor-dependent mechanisms during anti-CD20 antibody immunotherapy. J Exp Med 2004;199:1659–69.

26. Clynes RA, Towers TL, Presta LG, Ravetch JV. Inhibitory Fc receptors modulate *in vivo* cytoxicity against tumor targets. Nat Med 2000;6:443–6.

27. Weng WK, Levy R. Two immunoglobulin G fragment C receptor polymorphisms independently predict response to Rituximab in patients with follicular lymphoma. J Clin Oncol 2003;21:3940–7.

28. Sondermann P, Huber R, Oosthuizen V, Jacob U. The 3.2-A crystal structure of the human IgG1 Fc fragment-Fc γRIII complex. Nature 2000;406:267–73.

29. Cartron G, Dacheux L, Salles G, et al. Therapeutic activity of humanized anti-CD20 monoclonal antibody and polymorphism in IgG Fc receptor FcγRIIIa gene. Blood 2002;99:754–8.

30. Ghetie MA, Bright H, Vitetta ES. Homodimers but not monomers of Rituxan (chimeric anti-CD20) induce apoptosis in human B-lymphoma cells and synergize with a chemotherapeutic agent and an immunotoxin. Blood 2001;97:1392–8.

31. Epstein AL, Khawli LA, Hornick JL, Taylor CR. Identification of a tumor vessel-specific monoclonal antibody, TV-1, and its use to enhance the delivery of macromolecules to tumors after conjugation with interleukin 2. Cancer Res 1995;55:2673–80.

32. Epstein AL, Levy R, Kim H, et al. Biology of the human malignant lymphomas. IV. Functional characterization of ten diffuse histiocytic lymphoma cell lines. Cancer 1978;42:2379–91.

33. Ghetie MA, Podar EM, Ilgen A, et al. Homodimerization of tumor-reactive monoclonal antibodies markedly increases their ability to induce growth arrest or apoptosis of tumor cells. Proc Nat Acad Sci U S A 1997;94:7509–14.

34. Hornick JL, Hu P, Khawli LA, et al. chTNT-3/B, a new chemically modified monoclonal antibody directed against DNA for the tumor necrosis treatment of solid tumors. Cancer Biother Radiopharm 1998;13:255–68.

35. Frankel ME, Gerhard W. The rapid determination of binding constants for antiviral antibodies by a radioimmunoassay. An analysis of the interaction between hybridoma proteins and influenza virus. Mol Immunol 1979;16:101–6.

36. Sharifi J, Khawli LA, Hu P, King S, Epstein AL. Characterization of a phage display-derived human monoclonal antibody (NHS76) counterpart to chimeric TNT-1 directed against necrotic regions of solid tumors. Hybrid Hybridomics 2001;20:305–12.

37. Coloma MJ, Clift A, Wims L, Morrison SL. The role of carbohydrate in the assembly and function of polymeric IgG. Mol Immunol 2000;37:1081–90.

38. Deans JP, Li H, Polyak MJ. CD20-mediated apoptosis: signaling through lipid rafts. Immunology 2002;107:176–82.

39. Chan HT, Hughes D, French RR, et al. CD20-induced lymphoma cell death is independent of both caspases and its redistribution into triton X-100 insoluble membrane rafts. Cancer Res 2003;63:5480–9.

40. Camilleri-Broet S, Mounier N, Delmer A, et al. FcγRIIB expression in diffuse large B-cell lymphomas does not alter the response to CHOP+Rituximab (R-CHOP). Leukemia 2004;18:2038–40.

41. Byrd JC, Kitada S, Flinn IW, et al. The mechanism of tumor cell clearance by Rituximab *in vivo* in patients with B-cell chronic lymphocytic leukemia: evidence of caspase activation and apoptosis induction. Blood 2002;99:1038–43.

Clinical Cancer Research

Generation of Rituximab Polymer May Cause Hyper-Cross-linking–Induced Apoptosis in Non-Hodgkin's Lymphomas

Nan Zhang, Leslie A. Khawli, Peisheng Hu, et al.

Clin Cancer Res 2005;11:5971-5980.